

KAOLIN REFLECTANCE SPECTROSCOPY: USING PLS-R TO PREDICT CONTAMINANT CONTENT

Paulo Ricardo Nunes da Conceição ^{1*}

Carlos Otávio Petter ¹

Carlos Hoffmann Sampaio ²

Aaron Young ³

Abstract

The present study deals with the prediction of contaminant concentrations in kaolin using Partial Least Squares Regression (PLS-R). The aim is to show that PLS-R method can be used to predict contaminant concentration in kaolin. High level kaolin means a kaolin with high-brightness. Since brightness is directly related to the reflectance spectrum and kaolin contaminants affect the reflectance spectrum it is important to the beneficiation of kaolin relates optical features and contaminants. Depending on the product to be produced, the optical parameters will influence how the kaolin will be processed. High-brightness kaolin and two red and yellow inorganic pigments were used to simulate colours contaminants frequently found in Brazilian kaolins, such as, hematite, goethite, rutile and anatase. By adding different pigment concentrations to the pure kaolin, it was possible to create a small dataset containing the visible reflectance spectrum of each sample with the respective optical quality parameters of the kaolin. Results allow us to conclude that PLS-R can predict through the reflectance spectrum the contaminant concentration of the kaolin with R-squared equal 0.9954 for red content and R-squared equal 0.9973 for yellow one.

Keywords: Kaolin clays; Reflectance spectra; Brightness; Partial Least Squares.

ESPECTROSCOPIA DO CAULIM: USO DE PLS-R PARA PREDIZER O CONTEÚDO DE CONTAMINANTES

Resumo

O presente estudo trata da predição da concentração de contaminantes presentes no caulim através do uso de Partial Least Squares Regression (PLS-R). O objetivo é mostrar que PLS-R pode ser usada para prever o conteúdo de contaminantes no caulim. Para o caulim ser alto nível é preciso ter alta alvura. Como alvura está diretamente vinculada ao espectro de reflectância e este é afetado pelos contaminantes é importante para o processamento de caulim relacionar contaminantes com parâmetros ópticos. Os parâmetros ópticos do caulim influenciam como ele será produzido. Caulim de alta alvura e dois pigmentos inorgânicos amarelo e vermelho foram usados para simular contaminantes encontrados no caulim brasileiro, como, hematita, goetita, rutilo e anatásio. Adicionando diferentes concentrações de pigmento ao caulim puro, foi possível criar uma base de dados contendo o espectro de reflectância de cada amostra com seus respectivos parâmetros ópticos de qualidade. Conclui-se que PLS-R, através do espectro de reflectância, pode prever as concentrações dos contaminantes do caulim contaminado com R² igual a 0,9954 para contaminante vermelho e R² igual a 0,9973 para amarelo.

Palavras-chave: Caulim; Espectro de reflectância; Alvura; *Partial Least Squares*.

I INTRODUCTION

There are in the world many different types of industrial minerals, which are derived from different geological formations [1]. Among most widely used are talc, kaolin, mica,

barite, bentonite, quartz, diatomite, and calcium carbonate (natural and precipitated). Industrial minerals are applied to products and processes, such as raw materials or additives,

¹Laboratório de Processamento Mineral, Universidade Federal do Rio Grande do Sul – UFRGS, Porto Alegre, RS, Brasil. E-mail: paulo.conceicao@ufrgs.br

²Departament d'Enginyeria Minera, Industrial i TIC, Universitat Politècnica de Catalunya Barcelona Tech, Manresa, Barcelona, Spain.

³Department of Mining Engineering, University of Utah, Salt Lake City, USA.



in various industrial segments, such as ceramics, paints, paper, plastics, rubbers, fertilizers, cements and building materials. Industrial minerals are also called functional fillers because they reduce the consumption of more expensive raw materials and confer specific properties to the products according to the mineral filler used. Among the main properties of functional fillers, one can cite the optical properties that give visual appearance and are rigidly controlled. Kaolin is one of the most important clay-minerals and presents special characteristics. It is applied in the manufacture of paper, ceramics, paints, etc [2,3]. The main kaolin deposits in the world located in Georgia State (USA) and in the Amazon region, north of Brazil. Many of the kaolin impurities are associated with iron and titanium oxides [4-9]. Optical properties of kaolin are very important in most of its industrial applications [10]. In most cases, brightness is used as the optical comparison parameter, as well as the coordinates L^* , a^* and b^* [11]. Presence of impurities and contaminants such as hematite and goethite contribute significantly to the reduction of the brightness value [12,13]. Conventional analyses to determine the content of iron in kaolin use methods that are time consuming and generate chemical residues [14]. On the other hand, methods using, for example, visible spectroscopy associated with multivariate methods such as Partial Least Squares Regression (PLS-R) can provide fast and accurate results [15]. The aim of this study is to show that reflectance spectra in the visible light associated with multivariate regression method, in this approach, Partial Least Squares Regression (PLS-R) method, can be applied to predict the contaminant concentration values of kaolin based on their reflectance spectra.

1.1 Brightness

Brightness ISO is defined as the blue light reflectance corresponding to the spectral distribution with the specific wavelength of 457 nm for a perfectly diffuse surface (TAPPI T 535-om-03) [16]. It only considers the blue part of the spectrum, ignoring the yellow and red parts. When brightness is calculated by a colorimeter, only the length 457 nm is taken into consideration, otherwise, when using a spectrophotometer, a range of 400 to 500 nm (TAPPI standard T452-om-02) [17] is evaluated. Hence, it may be that the value of the whiteness does not represent what the human eye sees. Another important fact is that kaolin contaminants act on different parts of the reflectance spectrum because they have different colours. This turns out to be a disadvantage in the use of brightness as a parameter of quality or comparison [18,19].

The Equation 1 for calculating brightness follows the form:

$$\text{Brightness} = \frac{\sum(R(\lambda).F(\lambda))}{\sum F(\lambda)} \quad (1)$$

where $R(\lambda)$ = Reflectance values within the wavelength range 400 to 500 nm; $F(\lambda)$ = Values of the TAPPI function within the wavelength range 400 to 500 nm.

1.2 CIELAB

Colour is a matter of perception and subjectivity of interpretation. Avoiding problems, colour must be expressed objectively through numbers, thus ensuring that the final product conforms to its specifications. There are several colour measurement systems. The most commonly used colour system is the CIE (International Commission of Illumination). CIEL* a^* b^* or CIELAB in which there are three axes: L^* indication that varies from light (+) to dark (-), a^* indication that varies from red (+) to green (-), and b^* indication that varies from yellow (+) to blue (-), it is used to indicate that colour is perceived through reactions of the eye to sensations of opposite colours [19,20].

1.3 Partial Least Square Regression (PLS-R)

In data analysis, the goal is optimizing a performance criterion using example data or experience, learning and discovering some rules or properties from the given dataset [21,22]. Partial Least Square (PLS) is a multivariate data regression method for modelling relations between sets of observations by means of latent variables. According to Conceição [23] PLS is a multivariate regression method that relates the data matrix \mathbf{X} to a \mathbf{Y} response, which can be a singular \mathbf{y} (a response variable) or multiple \mathbf{Y} (more than one response variable). PLS is a powerful tool for finding the relationship between the matrix \mathbf{X} and the response matrix, particularly for datasets that have more variables than observations and in which the variables have noise and collinearity [24,25]. The regression equation to describe the response \mathbf{y} , as a linear combination of the matrix \mathbf{X} and the regression coefficients follows the Equation 2:

$$\mathbf{y} = \mathbf{XB} + \mathbf{F} \quad (2)$$

where \mathbf{F} is the remaining information that was not modelled; \mathbf{B} is the regression coefficient matrix.

PLS is a simple regression method to find the regression coefficients matrix, where the matrices of the data \mathbf{X} and \mathbf{Y} are decomposed into main components or latent variables. Conforming to Conceição [23] PLS modelling is also explained as a two-step process, developed simultaneously. In the first step, the two data blocks, \mathbf{X} and \mathbf{Y} , are decomposed into several factors, in this case known as latent variables, plus a residue matrix corresponding to the non-modelled data. Latent variables, such as the main components, can be represented as the product of the score and loading vectors or as the product of the matrices in which these vectors were grouped according to Equations 3 and 4.

$$\mathbf{X} = t_1 p_1' + t_2 p_2' + \dots + t_r p_r' + \mathbf{E} = \mathbf{TP}' + \mathbf{E} \quad (3)$$

$$Y = u_1q_1' + u_2q_2' + \dots + u_rq_r' + F = UQ' + F \quad (4)$$

Where **T** and **U** are scores matrices, **P** and **Q** are loadings matrices, and **X** and **Y** are the data blocks (**X**, instrumental measurements and **Y**, responses), and *r* is the number of latent variables. The matrices **E** and **F** are the residues associated with modelling and *r* is the number of principal components. The scores represent the coordinates of the samples in the main component system and loadings represent the relative contribution of each original variable to the formation of the same. In PLS there is a compromise between explaining the variance in **X** and obtaining the highest correlation with **Y** [25].

2 MATERIALS AND METHODS

2.1 Contaminants

Brightness and colour can be improved by several processes used by kaolin producers. Major contamination sources of kaolin are iron and titanium oxides that can cause the kaolin to have cream, pink or reddish coloration. The quantification and removal of these contaminants are fundamental for improvement the brightness and colour of kaolin. Artificial contaminants based on iron oxide with red and yellow coloration along with a sample of kaolin benefited of high brightness were used. In this way, contamination of each kaolin sample was strictly controlled. The purpose of using the red and yellow colours was to simulate the colours of the contaminants that are normally found in kaolin. The visible reflectance spectrum of the kaolin without contamination is different from the yellow and red contaminants and that difference is associated with the contamination concentration. The reflectance spectrum of red contaminant shows reflection in 600 nm to 700 nm range, otherwise, yellow contaminant shows reflection in 540 nm to 700 nm range (Figure 1).

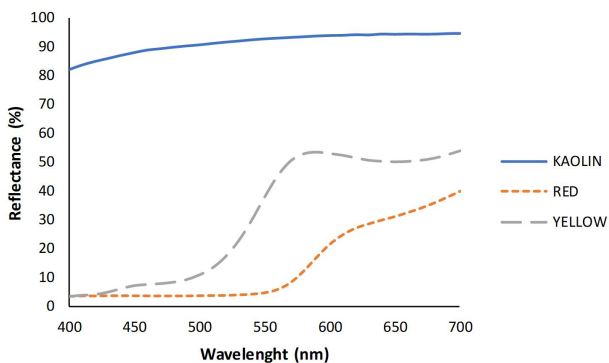


Figure 1. Spectrum of sample reflectance for the pure sample (KAO) and the yellow (YEL) and red (RED) contaminants. Red contaminant showing reflection in the 600 to 700 nm range and yellow showing reflection in the 540 nm to 700 nm range.

2.2 Experimental Procedure

The contaminants were added to the kaolin in two ways: a) red contaminant only (0.1% to 1%) and b) yellow contaminant only (0.1% to 1%). Six samples of kaolin were performed for each contraction of red and yellow contaminants at concentrations 0.1; 0.2%; 0.3%; 0.4%; 0.5%; 0.6%; 0.7%; 0.8%; 0.9%, and 1%. In total, there are 120 samples: 60 contaminated with yellow pigment and 60 with red contaminant, and three pure samples (kaolin, yellow pigment, and red pigment). After the contaminants were mixed with the kaolin pressed tablets of each mixture were made. The pellets were prepared by means of a metal cylinder, glass plate, and pneumatic press. The cylinder was placed on top of the glass plate and inside it the mixture of kaolin and contaminant was pressed. The surface in contact with the glass was used to measure the optical parameters of the mixture. Three measurements were made for each parameter and the value adopted for calculations was the average of these three measurements. A spectrophotometer Minolta model 2600d with optical system with spherical geometry $d/8^\circ$, standard illuminant D_{65} , and standard observer 10° was used to measure the reflectance spectra from the samples, and their colorimetric parameters (L^* , a^* and b^*). The spectrophotometer was calibrated using standards for white and black.

2.3 Multivariable Models

In order to generate the multivariable models, two data matrices were created. The first using matrix **X** to store the reflectance spectrum, L^* , a^* , b^* and brightness of the samples, and matrix **Y** to store the response variables (contaminant concentration). Before the models were created, the data was standardized (by subtracting the mean and then dividing by the standard deviation). In purpose of removing sources of undesirable variations of spectral data, the following pre-treatments were used: Kubelka-Munk transformation and multiplicative signal correction (MSC) to minimize the effects of light scattering; normalization to remove systematic variation and 1st derivative to correct baseline problems [26,27]. In the construction of the multivariate regression models, 116 reflectance spectra were used (four samples were left out), of which 78 spectra were used for calibration of the model and 38 spectra were used for external validation of the model. Capability of the calibration model to predict contaminant content based on spectra data was assessed using the prediction errors and correlation coefficients between the contaminant values estimated by the model using spectra and the reference values of the calibration set samples.

The number of latent variables (LV) in the construction of a PLS model is very important. In the determination of that number of LVs used in the model, a cross-validation (internal validation) was performed in the calibration set: a sample of the calibration set is excluded, the model was constructed, and its contaminant content was then estimated. The process was repeated until all samples are taken and PRESS [22] was computed. The models were developed with

PLS-2 in two stages: one for calculate de red contaminant and one for yellow contaminant. The multivariable models were created using The Unscrambler® software. Evaluating the performance of the numerical model against reference values, the error parameters used were:

a) Root Mean Squared Error (RMSE) [22]:

$$RMSE = \sqrt{\frac{\sum_{i=1}^n (y_i - \hat{y}_i)^2}{n-r-1}} \quad (5)$$

where n is number of samples and r is the number of latent variables.

The mean errors of the Root Mean Square Error of Calibration (RMSEC) and Root Mean Square Error of Prediction (RMSEP) were calculated from the RMSE (Equation 5). Measuring the calibration error, cross validation was used with the method called leave-one-out.

b) Correlation coefficients between the prediction and measured values were calculated for the calibration set, which were calculated as Equation 6, where \bar{y}_i is the mean of the reference measurement results for all samples in the training set [22].

$$R = \sqrt{1 - \frac{\sum_{i=1}^n (y_i - \hat{y}_i)^2}{\sum_{i=1}^n (y_i - \bar{y}_i)^2}} \quad (6)$$

3 RESULTS AND DISCUSSION

3.1 Colorimetric Parameters of the Samples

Concentrations ranging 0.1% to 1% of both contaminants were used to evaluate how the models would behave under conditions of contaminated samples and to model from low to high values. Using only samples with low concentrations of contaminants would make it impossible to predict samples with high contamination values. Figure 2 shows the evolution of the contamination on the kaolin spectrum by yellow (a) and red (b) contaminants, the higher the contamination, the greater the influence on the reflectance spectrum.

Reflectance spectra of pure kaolin, pure red contaminant and, pure kaolin mixed with the same concentrations of yellow and red contaminants are represented in the Figure 3. In the Figure 3, the way of each contaminant affects the spectrum of the kaolin is observed; red contaminant let its typical sign at wavelengths where the red colour has more influence, from 600 nm to 700 nm and a contaminant with yellow colouration is observed to act at wavelengths different from red. Yellow acts from 540 nm to 700 nm, also letting its presence well marked on the spectrum of kaolin. Still observing Figure 3, three spectra are observed, one for pure kaolin and the other two for pure kaolin mixed one with red and the other with yellow contaminant. The concentration of the yellow and red contaminants is equal, 0.1%. Equal concentrations of contaminants act differently in kaolin reflectance spectra. The influence

of the red contaminant, which could represent iron oxides such as hematite, goethite, limonite and magnetite, present in Brazilian kaolin, affects the brightness more significantly than the yellow contaminant that could represent impurities rich in titanium such as rutile and anatase. Pure kaolin spectrum had the optical parameters as follow: Brightness = 88.17, $L^* = 96.95$, $a^* = -0.05$, and $b^* = 3.29$. When contaminated with 0.1% of yellow the optical parameters were altered to Brightness = 83.57, $L^* = 96.17$, $a^* = 0.63$, and $b^* = 5.34$. Changing the contaminant for 0.15 of red, parameters changed to Brightness = 80.52, $L^* = 93.81$, $a^* = 3.07$ and, $b^* = 3.22$. When red is the contaminant it caused greater reduction in the brightness value than the reduction caused by the presence of the yellow one, at the same concentration. The explanation for this is that the colour of the sample is the result of a complex relationship between optical properties of the pigments and the kaolin matrix. These optical properties (index of refraction, absorption, transmission, diffusion, etc.)

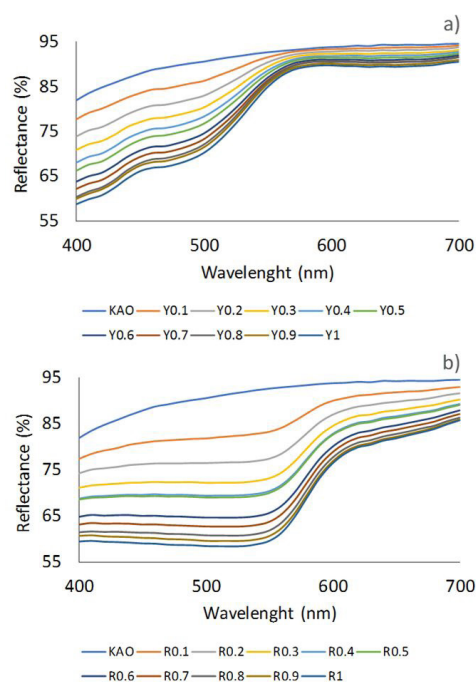


Figure 2. Reflectance spectrum of pure kaolin contaminated with pigment concentration (0.1% to 1%) of (a) yellow and (b) red pigment.

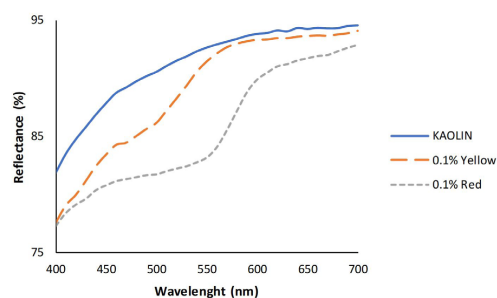


Figure 3. Reflectance spectrum of pure kaolin contaminated with the same concentration (0.1%) of red and yellow pigment.

are determined not only by the chemical nature but also by the size, shape and texture of each grain. Thus, properties of the red contaminant make its interaction with the kaolin less matt than the yellow contaminant.

3.2 Prediction of Contaminant Concentration

In mineral deposits, kaolin is associated with coloured contaminants and their quantification and removal is costly. Quantification of these contaminants is usually done through X-ray diffraction, X-ray fluorescence, Fourier transform infrared spectroscopy [28,29]. Another quick and inexpensive solution is the use of the Kubelka-Munk theory (K-M) that makes use of the reflectance spectrum of a sample.

K-M theory-based models relate reflectance to the scattering and light absorption of pigments. The proposal of this study is to apply a different approach from those models. The goal is the calculation of pigments content based only on the reflectance spectrum and on the mark left by each contaminant. It was used pre-treatments [25-27] to remove sources of undesirable variations of spectral data. The \mathbf{X} matrix was built with the transformed spectral data and mean centering and autoscaling were applied on the data. Number of LVs was chosen by comparing PRESS with LV and the LV number chosen was what minimized PRESS, in that case LV was 5.

3.2.1 Red and yellow content prediction

In purpose of multiple regression, it is very important to verify the collinearity between the input variables: reflectance spectrum, L^* , a^* , b^* and, Brightness. So that the relationship between them does not interfere in the results, causing erroneous or unreliable inferences. Verifying the existence and select the variables that would be excluded from the database, the leverage (h_i) value of the variables was used. Conforming to Esbensen et al. [26] leverage is directly related to the robustness of the model. The use of leverage indicated that the variables L^* , a^* , b^* and, brightness had high collinearity with the reflectance spectra. This can be explained by the fact that these parameters are calculated from the reflectance spectrum, therefore, in the study, only reflectance spectrum was used. Capability of the calibration model to predict contaminant content based on spectra data was assessed using the prediction errors (Equation 5) and correlation coefficients (Equation 6) between the contaminant values estimated by the model using only reflectance spectra and the reference values of the calibration set samples. According to the best PLS model using 5 latent variables the error parameters RMSEC equal 0.0996, SEC equal 0.1002, BIAS equal 0.006 and R squared equal 0.9782 for RED model and RMSEC equal 0.0754, SEC equal 0.0789, BIAS equal 0.001 and R squared equal 0.9876 for YELLOW model.

3.3 Validation

The calibration model for the prediction of red and yellow pigment content was validated by external validation. A set of 38 reflectance spectra were used. Figure 3 shows the good correlation between the values of the red pigment

content (a) and the yellow pigment (c) of the sample set and the experimental values for the samples used in the external validation set. The low dispersion of the predicted values around the regression line reveals a good model predictability. Observing figures (a) and (c) it is also possible to verify the high correlation between the values predicted by the proposed model and its reference values, demonstrating the absence of systematic errors in the results. The validation analysis showed that RMSEP equal 0.1283, SEP equal 0.1299, BIAS equal 0.0046 and R squared equal 0.9954 for RED model (a) and RMSEP equal 0.1091, SEP equal 0.1105, BIAS equal 0.0042 and R squared equal 0.9973 for YELLOW model (c). The results showed that PLS could interpret the nonlinear relationship between the matrix data \mathbf{X} and the response variables \mathbf{y} , in this case the red and yellow content.

Figure 4 also presents validation errors for red (b) and yellow models (d). The distribution of validation residuals for validation set demonstrates that the model is

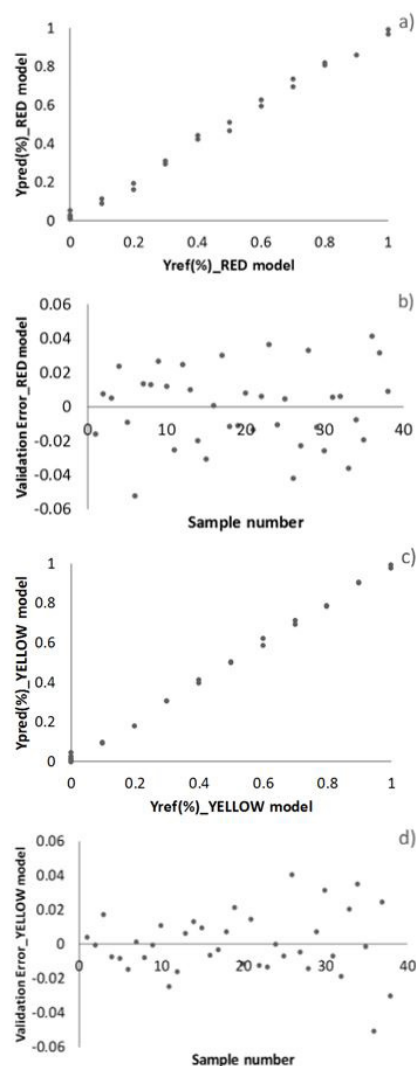


Figure 4. reference samples versus predicted samples for red (a) and yellow model (c) and, validation errors per sample for red (b) and yellow (d) model.

robust and presents a good fit. Validation errors presented low values for both models, however for the model with yellow contaminant, the values of greater contamination presented the biggest errors.

4 CONCLUSIONS

Kaolin is a very important clay mineral in several industrial segments and its optical properties are highly valued. In this study the use of Partial Least Squares (PLS) method for determination of contaminant concentration of kaolin, contaminated by red and yellow pigments. These pigments simulated frequent elements that could contaminate Brazilian kaolin clays, such as hematite, goethite and rutile, giving them different colour aspects. A database was constructed where the colorimetric response or the optical parameters were directly related to the contaminant content added to the pure kaolin. The use of the reflectance spectrum brings much larger amount of information about the contaminants than just the brightness value. The contaminants had different colours so that the phenomena of absorption and scattering of light were also different and affected the reflectance spectrum of

kaolin at different wavelengths. Partial Least Squares method managed to capture the changes that contaminants cause in the reflectance spectrum of pure kaolin. Using PLS, it was possible to correlate the contaminant-modified reflectance spectrum with the pigment content. Moreover, PLS is suitable, to some extent, to obtain a multiple regression model for treat collinear spectroscopic data and predict coloured pigments concentration, overcoming some overfitting contamination effects. In conclusion, results allow us to assert that PLS-R can predict through the reflectance spectrum the contaminant concentration of the kaolin with RMSEP equal 0.1283 and R-squared equal 0.9954 for red content, and RMSEP equal 0.1091 and R-squared equal 0.9973 for yellow one. In addition, PLS is a powerful tool to aid in the prediction of the colorimetric contaminant of kaolin.

Acknowledgements

The authors would like to thank Federal University of Rio Grande do Sul (UFRGS) and National Council of Technological and Scientific Development (CNPq) to support the research.

REFERENCES

- 1 Luz AB, Lins FAF. Rochas e minerais industriais: usos e especificações. Rio de Janeiro: CETEM/MCT; 2008.
- 2 Murray HH. Traditional and new applications for kaolin, smectite, and palygorskite: a general overview. *Applied Clay Science*. 2000;17(5-6):207-221. [http://dx.doi.org/10.1016/S0169-1317\(00\)00016-8](http://dx.doi.org/10.1016/S0169-1317(00)00016-8).
- 3 Murray HH. *Applied clay mineralogy: occurrences, processing and application of kaolins, bentonites, palygorskite-sepiolite, and common clays*. Amsterdam: Elsevier; 2007. p. 85-109.
- 4 Montes CR, Melfi AJ, Carvalho A, Vieira-Coelho AC, Formoso MLL. Genesis, mineralogy and geochemistry of kaolin deposits of the Jari River, Amapá State, Brazil. *Clays and Clay Minerals*. 2002;50(4):494-503. <http://dx.doi.org/10.1346/000986002320514217>.
- 5 Pruetz RJ. Kaolin deposits and their uses: Northern Brazil and Georgia, USA. *Applied Clay Science*. 2016;131:3-13. <http://dx.doi.org/10.1016/j.clay.2016.01.048>.
- 6 Santos E, Scorzelli RB, Bertolino LC, Alves OC, Munayco P. Characterization of kaolin from the Capim River region - Brazil. *Applied Clay Science*. 2012;55:164-167. <http://dx.doi.org/10.1016/j.clay.2011.11.009>.
- 7 Santos AEA Jr, Rossetti DF, Murray HH. Origins of the Rio Capim kaolinites (northern Brazil) revealed by $\delta^{18}\text{O}$ and δ^{D} analyses. *Applied Clay Science*. 2007;37(3-4):281-294. <http://dx.doi.org/10.1016/j.clay.2007.01.005>.
- 8 Silva FANG, Luz AB, Sampaio JA, Bertolino LC, Scorzelli RB, Duttine M, et al. Technological characterization of kaolin: Study of the case of the Borborema-Seridó region (Brazil). *Applied Clay Science*. 2009;44(3-4):189-193. <http://dx.doi.org/10.1016/j.clay.2009.01.015>.
- 9 Sousa DJL, Varajão AFDC, Yvon J, Scheller T, Moura CAV. Ages and possible provenance of the sediments of the Capim River kaolin, northern Brazil. *Journal of South American Earth Sciences*. 2007;24(1):25-33. <http://dx.doi.org/10.1016/j.jsames.2007.02.007>.
- 10 Bertolino LC, Rossi AM, Scorzelli RB, Torem ML. Influence of iron on kaolin whiteness: an electron paramagnetic resonance study. *Applied Clay Science*. 2010;49(3):170-175. <http://dx.doi.org/10.1016/j.clay.2010.04.022>.
- 11 Castellano M, Turturro A, Riani P, Montanari T, Finocchio E, Ramis G, et al. Bulk and surface properties of commercial kaolins. *Applied Clay Science*. 2010;48(3):446-454. <http://dx.doi.org/10.1016/j.clay.2010.02.002>.
- 12 Chandrasekhar S, Ramaswamy S. Influence of mineral impurities on the properties of kaolin and its thermally treated products. *Applied Clay Science*. 2002;21(3-4):133-142. [http://dx.doi.org/10.1016/S0169-1317\(01\)00083-7](http://dx.doi.org/10.1016/S0169-1317(01)00083-7).

- 13 Garcia AG, Buxton M. Visible and infrared reflectance spectroscopy for characterization of iron impurities in calcined kaolin clays. In: Proceedings of the Optical Characterization of Materials Conference (OCM 2015); 2015. Karlsruhe: KIT Scientific Publishing; 2015. p. 215-226.
- 14 Hunter RS, Harold RW. The measurement of appearance. 2nd ed. New York: John Wiley & Sons; 1987.
- 15 Morgano MA, Faria CG, Ferrão MF, Bragagnolo N, Ferreira MMC. Determinação de proteína em café cru por espectroscopia NIR e regressão PLS. Food Science and Technology. 2005;25(1):25-31. <http://dx.doi.org/10.1590/S0101-20612005000100005>.
- 16 American National Standards Institute. TAPPI T 535-OM-03: brightness of clay and other mineral pigments (D/0 DIFFUSE). Washington: ANSI; 2003.
- 17 American National Standards Institute. TAPPI T 452 OM-02: brightness of pulp, paper, and paperboard (directional reflectance at 457 nm). Washington: ANSI; 2002.
- 18 Nayatani Y, Sobagaki H. Relationship between brightness/luminance ratio and additivity-law failure. Color Research and Application. 2002;27(3):185-190. <http://dx.doi.org/10.1002/col.10045>.
- 19 Hunter RS, Harold RW. The measurement of appearance. 2nd ed. New York: John Wiley & Sons; 1987.
- 20 Melville MD, Atkinson G. Soil colour: Its measurement and its designation in models of uniform colour space. European Journal of Soil Science. 1985;36(4):495-512. <http://dx.doi.org/10.1111/j.1365-2389.1985.tb00353.x>.
- 21 Alpaydin E. Introduction to machine learning. 2nd ed. Massachusetts Institute of Technology; 2010. 579 p.
- 22 Esbensen KH. Multivariate data analysis: in practice. 4th ed. CAMO; 2000. 600 p.
- 23 Conceição PRN. Utilização de análise multivariada de dados na otimização de misturas de minerais industriais para a formulação de tintas [tese]. Porto Alegre: PPGEM/UFRGS; 2006.
- 24 Conceição PRN, Petter CO, Sampaio CH. Prediction of water-based paint properties based on their mineral fillers: Simplex-PLSR coupling application. HOLOS. 2018;34(2):2-15.
- 25 Wold S, Sjostrom M, Eriksson L. PLS-regression: a basic tool of chemometrics. Chemometrics and Intelligent Laboratory Systems. 2001;58(2):109-130. [http://dx.doi.org/10.1016/S0169-7439\(01\)00155-1](http://dx.doi.org/10.1016/S0169-7439(01)00155-1).
- 26 Esbensen KH, Guyot D, Westad F, Houmoller LP. Multivariate data analysis in practice: an introduction to multivariate data analysis and experimental design. 5th ed. Oslo: CAMO; 2002. 598 p.
- 27 Esbensen K, Geladi P. Strategy of Multivariate Image Analysis (MIA). Chemometrics and Intelligent Laboratory Systems. 1987;7:67-86.
- 28 Sales PFS. Estudo dos tratamentos químico e térmico na caulinita e a influência na remoção de contaminantes em efluentes de mineração [dissertação]. Lavras: Universidade Federal de Lavras; 2011.
- 29 Gonçalves IG. Determinação da concentração de contaminantes no caolim através da Teoria de Kubelka-Munk [dissertação]. Porto Alegre: Universidade Federal do Rio Grande do Sul; 2009.

Recebido em: 11 Jul. 2018

Aceito em: 30 Oct. 2018